



## A study of JET carbon impurity sources

J.D. Strachan<sup>a,b,\*</sup>, G. Corrigan<sup>a</sup>, M. Stamp<sup>a</sup>, J. Spence<sup>a</sup>, J. Zacks<sup>c</sup>, JET-EFDA Contributors<sup>a,1</sup>

<sup>a</sup>JET-EFDA Culham Science Centre OX14 3DB, Abingdon, UK

<sup>b</sup>PPPL Princeton University, Princeton, NJ 0854, USA

<sup>c</sup>Queen's University of Belfast, University road, Belfast, BT7, UK

### ARTICLE INFO

PACS:  
52.25.Vy

### ABSTRACT

This paper compares experimental JET carbon and hydrogen visible emission to EDGE2D/NIMBUS calculations. The calculations themselves indicate that: (1) the integrated deuterium ionization in the SOL is proportional to the  $D_{\alpha}$  chordal integrated photon flux, (2) the carbon ionization in the SOL or the divertor is proportional to the calculated CIII chordal light, and (3) the ratio of line integrated photon fluxes from a vertical chord to a horizontal chord indicates whether the main chamber SOL content originated primarily from a wall source or from ion flow out of the divertor. Comparison was made to both inter-ELM H-Mode and L-Mode JET gas box divertor plasmas. The calculations infer that the experimental core contamination was caused by carbon sputtering arising primarily from the main chamber. The experimental, main chamber carbon yield was 1–4% in L-Mode and 5–10% in the inter-ELM H-Mode period.

Published by Elsevier B.V.

Erosion, migration, and contamination phenomena are important issues for a fusion reactor. However, understanding these issues on present machines is difficult. One difficulty is ambiguity about the location and magnitude of impurity sources [1]. In this paper, JET carbon impurity sources are studied indicating that the main chamber wall source dominates the core contamination. This finding is different than previous JET results [2] based upon methane screening experiments, probably indicating that those measurements were influenced by divertor leakage of injected methane.

In a sufficiently large diverted tokamak, the impurity ions are calculated to contaminate the core by first contaminating the main chamber SOL, and subsequently, transporting across the field lines into the core [3]. Direct impurity neutral penetration and impurity ionization in the core is negligible at separatrix temperatures above about 50 eV. The SOL can be contaminated by two mechanisms;

1. ionization in the SOL from impurity neutrals generated at the main chamber wall. This release is imposed by neutral bombardment from escaping charge exchange neutrals from the core as well as ion bombardment which can be enhanced by SOL turbulence,

2. ion out flux from the divertor of impurities sputtered near the outer strike point. Direct neutral escape from the divertor is thought to be small since the mean free path for impurity ionization is typically much smaller than the divertor size [3].

EDGE2D/NIMBUS is used to interpret the JET experimental CIII (465 nm) and  $D_{\alpha}$  spectroscopic signals in terms of the spatial origin of the deuterium and carbon ionization in the main chamber SOL. EDGE2D indicates that the carbon source is dominated by main chamber sources.

The JET plasmas were described in the JET carbon screening experiments (see Sections 2.3 and 3.3 of Ref. [2]). These include the L-Mode and inter-ELM H-Mode plasmas with the JET MKGB Divertor (July 1998 to March 2001). Both of these plasma types are free of ELMs and thus avoid the complications that ELMs present to the spectroscopic signals.

These plasmas include all the available MKGB plasmas having plasma current >1.5 MA, main chamber clearance >5 cm, neutral beam heating (1.5–8 MW), and toroidal magnetic field >1.5 T. ICRF heating was not studied since such plasmas might have an additional impurity source in the vicinity of the RF antennae. Also, the data base was restricted to plasmas with moderate triangularity ( $\delta < 0.4$ ) avoiding impurity sources from the top of the machine, where the second X-point (being just outside the vessel) draws plasma contact to that region. 108 L-Mode and 41 inter-ELM plasmas achieved these criteria. The L-Mode plasmas had either 1.85 or 2.35 MA. The inter-ELM plasmas had ELM periods longer than 0.6 s isolating a distinct inter-ELM time phase.

\* Corresponding author. Address: PPPL Princeton University, Princeton, NJ 0854, USA.

E-mail address: [jstrachan@pppl.gov](mailto:jstrachan@pppl.gov) (J.D. Strachan).

<sup>1</sup> See appendix of M.L. Watkins, et al., Fus. Energ. 2006 (21st IAEA Int. Conf. Chengdu).

This data set was used previously [2] to conclude that core contamination by divertor impurity sources was significant. That conclusion relied upon the methane screening data from divertor locations was influenced by previously unknown leakage from the methane gas injection module [4]. The leakage allowed some of the divertor injected methane to escape directly into the main chamber making the fuelling efficiency (core contamination) of divertor carbon sources appear higher than probably occurred.

EDGE2D/NIMBUS [5] is a SOL boundary code designed specifically for single null JET plasmas. It has been used to understand a variety of phenomena. The charged particles are described by the fluid conservation equations for density, parallel momentum, and energy while the neutral particles (deuterium and carbon) are described by the Monte Carlo code NIMBUS. The principal limitation is the lack of hydrocarbons since the carbon is introduced as atoms. A further limitation is that spatially constant transport coefficients without pinches are generally used. Also, drifts were not used in these calculations.

The approach [3] in this paper is to form an ensemble of EDGE2D runs for which many of the input parameters are individually changed. In this manner, the calculations encompass variations in the experimental data. The parameter variations included the carbon diffusion coefficient ( $0.2\text{--}1\text{ m}^2/\text{s}$ ), the deuterium diffusion coefficient ( $0.2\text{--}1\text{ m}^2/\text{s}$ ), the electron and ion thermal conductivities ( $0.2\text{--}1\text{ m}^2/\text{s}$  and assumed to be equal), the SOL power ( $2\text{--}10\text{ MW}$ ), the edge density ( $n_{\text{sep}} = 0.8\text{--}1.2 \times 10^{19}/\text{m}^3$ ), and the initial carbon energy ( $0.1\text{--}10\text{ eV}$ ). Variation of the deuterium gas injection rate caused the density variation.

Three calculation ensembles were formed with different carbon sources:

1. An outer strike point source of injected carbon was used to identify effects due to divertor sources. This source extended 5 cm above the outer vertical target.
2. A sputtering carbon source was also used which originated due to deuterium and carbon bombardment of the carbon walls and targets. Physical sputtering was always included, while chemical sputtering was considered using various chemical sputtering coefficients [6–12]. Cases with physical sputtering only were also part of this ensemble.
3. A uniform wall source of injected carbon was used to identify effects due to wall sources. This source did not extend into the divertor. The variations for the uniform wall source were fewer since the SOL carbon ionization fraction was insensitive to the SOL transport coefficients.

The poloidal distribution of the carbon ionization for the three calculation ensembles was correlated with the different carbon source locations. When the assumed source was located at the outer strike point, there was little carbon ionization calculated in the main chamber SOL. On the other hand, when the source is located uniformly in the main chamber, then the carbon ionization is calculated to be entirely in the main chamber SOL. The assumed sputtered source produced a calculated carbon ionization pattern that was a combination of the calculated outer strike point source and the uniform wall sources.

On each EDGE2D calculation in the ensemble, the spectroscopic signals (Fig. 1) were simulated [13] according to the charge states calculated by the ADAS coefficients for the plasmas along the experimental diagnostic sight-lines. The sight-lines of the JET CIII and  $D_\alpha$  spectroscopic signals that were most useful in this study

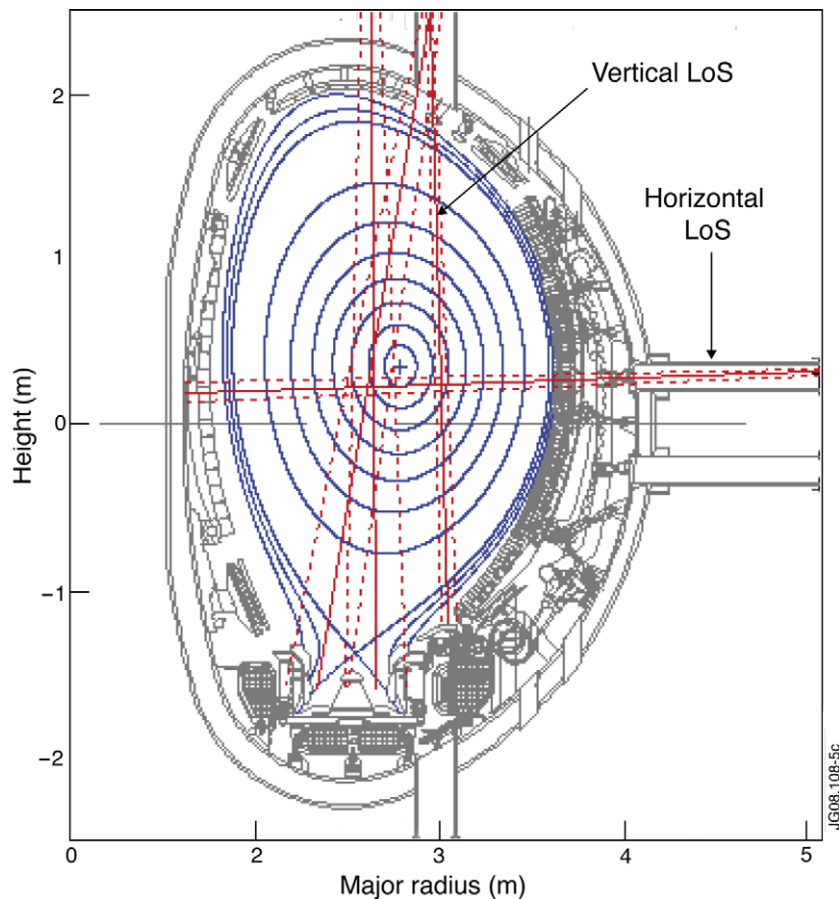


Fig. 1. Poloidal cross-section of JET with the sight-lines of the spectroscopic signals indicated. The vertical signal terminates outside the divertor at larger major radius.

were (1) the horizontal view, (2) the vertical view that did not include the divertor, and (3) the wide angle view of the entire divertor [14]. The CIII excitation was calculated to be almost entirely due to electron impact, with charge exchange commonly forming a 5% contribution and recombination typically forming a 0.5% contribution. Notice that detached cases were not part of any calculation.

The EDGE2D/NIMBUS calculations indicated that the calculated 465 nm CIII spectral line viewing the plasma horizontally near the mid-plane is proportional to the calculated integrated carbon ionization rate in the main chamber SOL. Regression to the ensemble (Fig. 2) of sputtered EDGE2D calculations indicates:

$$Sc = 2.3 \times 10^7 C3H \quad (1)$$

$Sc$  is the total volume integrated ionization rate (per second) of carbon in the main chamber SOL, while  $C3H$  is the line integrated intensity of the CIII 465 nm spectral line along the horizontal sight-line measured in photons/str/cm<sup>2</sup>/s as in Fig. 3. The underlying assumption is that the local emission arises entirely from the SOL and is not influenced by nearby vessel structure. Fig. 2 indicates that the EDGE2D calculated CIII light is a good indicator of carbon ionization rate independent of the SOL transport coefficients, the sputtering yield, or the carbon source. The assumed uniform wall source of carbon in EDGE2D resulted in about 40% more CIII light per carbon ionization than the intrinsic sputtering sources. On the other hand, the assumed outer strike point source produces 10–100 times less calculated main chamber SOL carbon ionization and correspondingly less CIII light.

The vertical CIII signal which views outside of the divertor on the large major radius side (Fig. 1) is also calculated to be proportional to the carbon ionization in the main chamber SOL but additionally has a dependence upon carbon ions flowing out of the divertor into the sight-line. For a uniform EDGE2D wall source, the vertical and horizontal channels yield similar calculated signals (Fig. 3) even though the SOL volume seen by the vertical channel is larger. However, for EDGE2D outer strike point sources and for sputtered carbon sources, the vertical signal is calculated to be

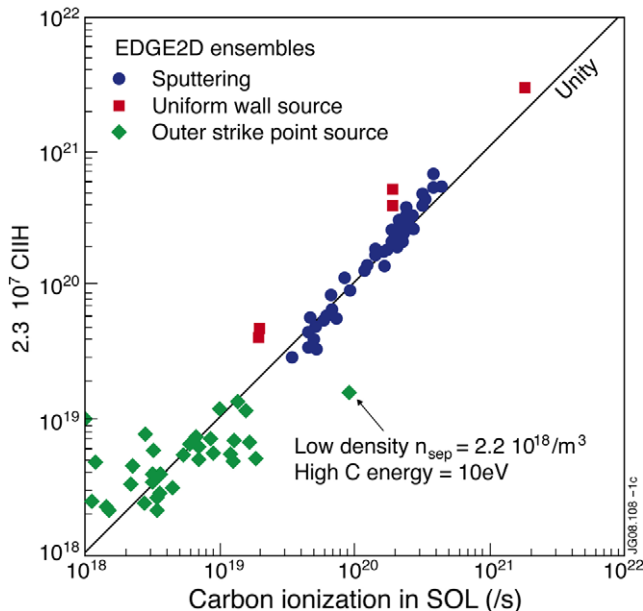


Fig. 2. The carbon ionization in the SOL as indicated by Eq. (1) and thus estimated from the calculated line integral spectroscopy is plotted against the actual EDGE2D calculated SOL ionization for each ensemble: the uniform wall (square), the outer strike point (diamond), and the sputtered (circle) sources. Each data point originated from a separate EDGE2D calculation.

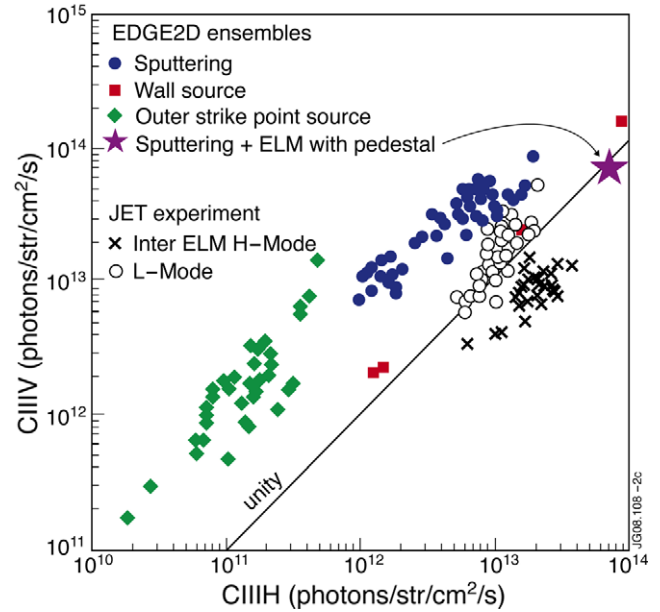


Fig. 3. The CIIIV (line integral vertical) signal is plotted against the CIIIH (line integral horizontal) signal. The EDGE2D calculations are indicated by solid points for the three sources as in Fig. 2 and the star point is a calculation with an H-Mode pedestal and ELMs at an inter-ELM time. JET experimental results are hollow circles L-Mode and crosses for JET inter-ELM H-Mode.

about 10 times larger than the horizontal signal. EDGE2D is indicating that the carbon ions originating in the divertor are accelerated by the thermal force into the line-of-sight of the vertical spectrometer, enhancing this signal. The experimental JET L-Mode data has a ratio of vertical to horizontal CIII signals that is in agreement with a uniform wall source with no indication of any signal enhancement due to ions being extracted from the divertor (Fig. 3). The inter-ELM H-Mode data indicates a further factor-of-two enhancement of the experimental horizontal signal as if to indicate that the experimental carbon source is more oblate than uniform and is more strongly located near the mid-plane. For the EDGE2D calculations, the SOL transport coefficients were spatially constant, so a single EDGE2D sputtering case was calculated with an H-Mode pedestal and ELMs [15]. The spectral signals were calculated inter-ELM indicating a factor of 2–3 higher calculated CIIIH/CIIIV signal (star point in Fig. 3) so that the difference between experimental H-Mode and L-Mode is likely due to a difference in time evolution and pedestal.

Following the logic of Fig. 2, the relationship of the integrated deuterium ionization to the  $D_\alpha$  signal was explored using EDGE2D (Fig. 4). The horizontal viewing  $D_\alpha$  signal (FLW is the toroidal integral assuming toroidal symmetry) was calculated to be a good indicator of the deuterium ionization rate in the main chamber SOL. Regression indicates:

$$SDw = 24 \times FLW \quad (2)$$

$SDw$  is the calculated volume integrated deuterium ionization rate (per second) from the wall. The number 24 is in the range of the classic Johnson-Hinnov factor, 15, and might be higher due to molecular processes or high temperature effects [16].

Since these calculations are in steady-state, the deuterium ionization (source rate) is also the deuterium loss rate to the main chamber walls, which therefore can be used to calculate the carbon sputtering yield from the main chamber walls and also the sputtering yield from the divertor. Thus, using Eq. (1) with Eq. (2) produces an EDGE2D formula for the carbon sputtering yield in terms of the spectroscopically measured CIII and  $D_\alpha$  light.

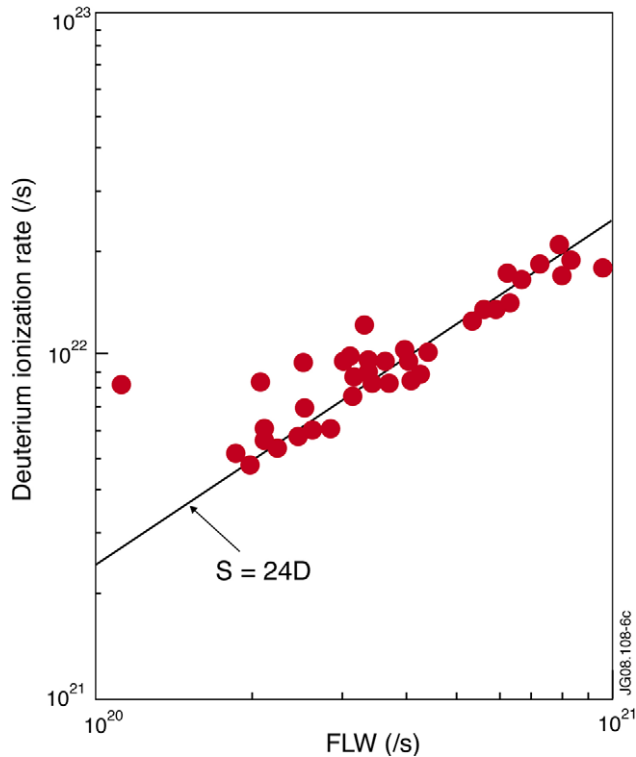


**Fig. 4.** The volume integrated deuterium ionization rate in the main chamber from EDGE2D is plotted against the volume integrated  $D_\alpha$  emission.

This spectroscopic definition is a good indicator ( $\sim 10\%$  high with 5% standard deviation) of the EDGE2D calculated ratio of carbon to deuterium ionization. Since these cases are from the ensemble of calculated sputtered cases, the 15% scatter represents the sensitivity to input parameter variation. The good agreement indicates that the use of the spectroscopic signals to determine the averaged carbon sputtering yield is a good approximation. Also, this good fit indicates that effects such as neutral deuterium penetration to the core, from the divertor to the main chamber, and into the pump are calculated to be negligible.

The experimental main chamber carbon sputtering yield is approximately equal to  $\frac{1}{2}$  the Haasz value [10] as is usually obtained in JET studies [6] (Fig. 5). The L-Mode experimental sputtering yield is about five times larger than that calculated solely from physical sputtering. Thus, chemical sputtering is required in order to achieve the observed main chamber CIII signals. The principal L-Mode experimental dependence was upon the density decreasing from about 4% at a separatrix density of  $5 \times 10^{18}/\text{m}^3$  to 1.5% at  $1.2 \times 10^{19}/\text{m}^3$ . This decrease was about twice the calculated decrease expected from the Haasz sputtering coefficient which decreases from 3% to 2%. Experimentally, the inter-ELM H-Mode plasmas have a factor-of-two higher sputtering yields which was not correlated to the applied power, the plasma current, or the beam energy. Again, the inter-ELM H-Mode EDGE2D calculation also had a factor-of-two higher sputtering yields than L-Mode (star point in Fig. 5). This indicates that time evolution and pedestal effects which might bring more energetic CX neutrals onto the wall are a possibility to explain the larger sputtering yield.

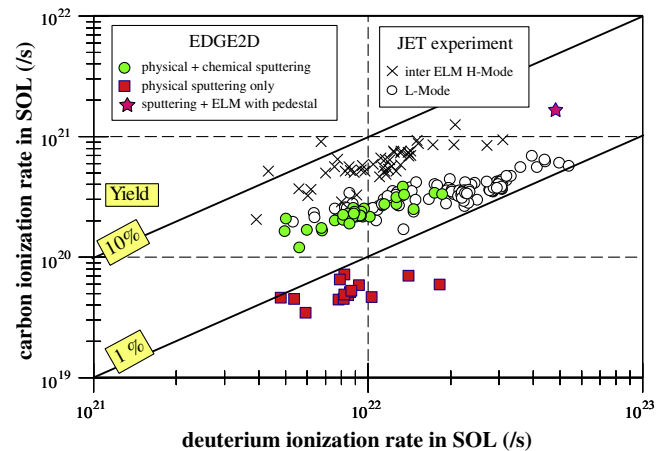


**Fig. 5.** The volume integrated carbon ionization rate in the SOL is plotted against the volume integrated deuterium SOL ionization rate. The experimental symbols are the same as for Fig. 3. The EDGE2D calculations all arise from the sputtering ensemble of Fig. 3. The red squares have only physical sputtering while the green circles include also chemical sputtering. The star is an EDGE2D calculation which includes an H-Mode pedestal.

In conclusion, the modeling of the impurity sources for these plasmas agrees with previous JET modeling of the magnitude of the carbon sputtering coefficients. The inference of a predominately wall source of carbon in JET plasmas (Fig. 3) contrasts with the methane screening experiments [2]. Those experiments were influenced by a leakage path for the injected gas into the main chamber SOL [4]. This paper confirms that ion escape out of the Gas Box divertor was not observed and that wall sources probably dominate the JET core contamination, at least in the absence of ELMs.

### Acknowledgement

This work, supported by the European Communities, was carried out within the framework of the European Fusion Development Agreement. The views and opinions expressed herein do not necessarily reflect those of the European Commission. JDS was supported by US DOE.

### References

- [1] A. Loarte et al., Nucl. Fus. 47 (2007) S203.
- [2] J.D. Strachan et al., Nucl. Fus. 43 (2003) 922.
- [3] J.D. Strachan et al., Nucl. Fus. 44 (2004) 772.
- [4] J.D. Strachan, et al., in: Proceedings of 33rd EPS Conference on Contribution Fusion and Plasma Physics, vol. 31F, Warsaw, Poland, p. 1.30.
- [5] R. Simonini et al., Contribution Plasma Phys. 34 (1994) 368.
- [6] H.Y. Guo et al., Nucl. Fus. 40 (2000) 379.
- [7] J. Roth, J. Nucl. Mater. 266–269 (1999) 51.
- [8] A.A. Haasz, B.V. Mech, J.W. Davis, J. Nucl. Mater. 231 (1996) 170.
- [9] A. Pospieszczyk et al., J. Nucl. Mater. 241–243 (1997) 883.
- [10] A.A. Haasz, J.W. Davis, J. Nucl. Mater. 224 (1995) 141.
- [11] C. Garcia-Rosales, J. Roth, in: Proceedings of 21st EPS Conference on Contribution Fusion and Plasma Physics, Montpellier, p. II-770, 1994.
- [12] V. Philipps et al., J. Nucl. Mater. 313–316 (1997) 354.
- [13] C.F. Maggi, J. Nucl. Mater. 266–269 (1999) 867.
- [14] M. Stamp et al., J. Nucl. Mater. 266–269 (1999) 685.
- [15] A. Kallenbach et al., Plasma Phys. Control. Fus. 46 (2004) 431.
- [16] S. Brezinsek et al., Plasma Phys. Control. Fus. 47 (2005) 1.